

# Influence of additive content on the anisotropy in hot-pressed $\text{Si}_3\text{N}_4$ ceramics using grain orientation measurements

C. Santos<sup>a,\*</sup>, K. Strecker<sup>a</sup>, S.A. Baldacim<sup>b</sup>, O.M.M. da Silva<sup>b</sup>, C.R.M. da Silva<sup>b</sup>

<sup>a</sup> Departamento de Engenharia de Materiais DEMAR-FAENQUIL, Polo Urbo-industrial, Gleba AI-6, s/n, Cep. 12600-000 Lorena, SP, Brazil

<sup>b</sup> Centro Técnico Aeroespacial, Divisão de Materiais AMR-CTA, Pça. Marechal do Ar Eduardo Gomes, 50, Cep. 12228-904 S.J. Campos, SP, Brazil

Received 27 March 2003; received in revised form 15 May 2003; accepted 10 July 2003

## Abstract

The influence of additive content on the microstructure and its mechanical properties in planes parallel and normal to the hot-pressing axis of  $\text{Si}_3\text{N}_4$  ceramics has been investigated by direct measurement of the grain orientation from SEM micrographs and orientated Vicker's indentations. It is shown that an increasing additive content leads to a microstructure with grains of higher aspect ratios, resulting in an increase of the fracture toughness. Furthermore, the difference in mechanical anisotropy between the planes parallel and normal to the hot-pressing directions is gradually reduced with increasing additive content, due to the smaller degree of orientation of the elongated  $\beta\text{-Si}_3\text{N}_4$  grains in the plane parallel to the hot-pressing direction.

© 2003 Elsevier Ltd and Techna Group S.r.l. All rights reserved.

**Keywords:** A. Hot pressing; D.  $\text{Si}_3\text{N}_4$ ; Anisotropy; Characterization; Fracture toughness

## 1. Introduction

One key issue of high quality and reliable structural  $\text{Si}_3\text{N}_4$ -based ceramics is a high fracture toughness which can be achieved by the combination of several factors such as: use of high quality starting powders, optimization of the processing parameters thus reducing the frequency and the size of defects, the production of grains with high aspect ratios and control of the interfacial bonding strength between the  $\beta\text{-Si}_3\text{N}_4$  grains and the intergranular phase [1–3]. Improvement of the aforementioned parameters led to  $\text{Si}_3\text{N}_4$  ceramics which routinely exhibit fracture toughness values higher than  $6\text{ MPa m}^{1/2}$ . More recently, Becher et al. [4] and Kanzaki et al. [5] achieved even higher fracture toughness by adding small quantities of  $\beta\text{-Si}_3\text{N}_4$  to the starting powder mixtures, acting as seeds, to facilitate the  $\alpha$ - to  $\beta\text{-Si}_3\text{N}_4$  phase transformation and resulting in large  $\beta\text{-Si}_3\text{N}_4$  grains of high aspect ratio embedded in a matrix of smaller  $\beta\text{-Si}_3\text{N}_4$  grains, that produced high fracture toughness, around  $9\text{--}10\text{ MPa m}^{1/2}$ .

The high fracture toughness of  $\text{Si}_3\text{N}_4$ -based ceramics is the result of their microstructure, consisting of high aspect ratio  $\beta\text{-Si}_3\text{N}_4$  grains, diffculting the crack-propagation principally by the crack bridging and crack deflection mechanisms [6–11]. According to these studies, fracture toughness increases with increasing aspect ratio and volume content of these grains.

One of the principal aspects affecting  $\text{Si}_3\text{N}_4$  ceramics produced by hot-pressing is the microstructural anisotropy of these materials [12–14]. These microstructural variations lead to anisotropic mechanical properties, due to the preferential orientation of the elongated  $\beta\text{-Si}_3\text{N}_4$  grains perpendicular to the hot-pressing direction [12,13], which in some cases results in a variation of up to 50% in the fracture toughness in the directions longitudinal and transversal to the hot-pressing axis [15].

In the present work, fracture toughness has been determined by the crack length of Vicker's indentations [16]. The variation of the fracture toughness due to the anisotropy of the hot-pressed  $\text{Si}_3\text{N}_4$  ceramics has been investigated in planes parallel and normal to the hot-pressing direction, using different indentation angles. The results are presented in relation to the additive content. Furthermore, this work emphasizes the determination of the anisotropy by simple, direct and reliable observation technique of the grains orienta-

\* Corresponding author. Tel.: +55-12-31599900/39476414;  
fax: +55-12-31533006.

E-mail addresses: claudinei@ppgem.faelnquil.br, clvr2@yahoo.com (C. Santos).

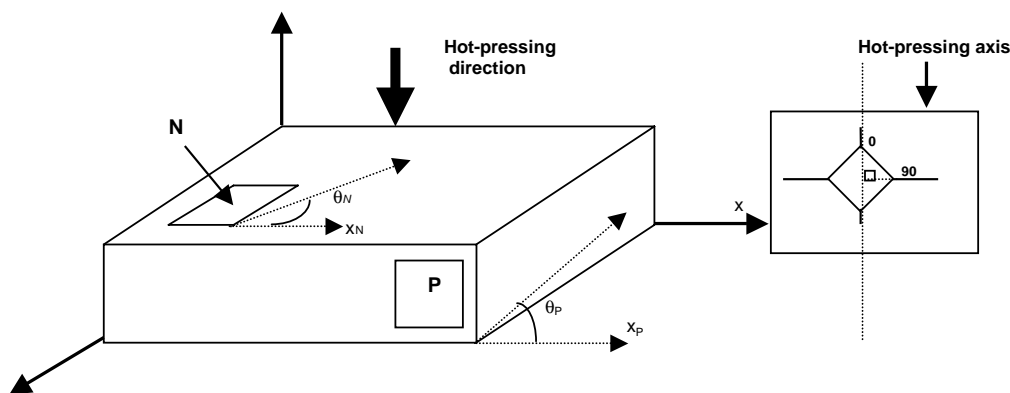


Fig. 1. Schematic figure of toughness anisotropy measurements by oriented Vicker's indentations in an uniaxially hot-pressed specimen. Two different planes were analyzed in the experiments: (i) crack plane normal to the hot-pressing direction (N) and (ii) parallel to the hot-pressing direction (P).  $\theta_N$ , grain orientation angle related to the N plane;  $\theta_P$ , grain orientation angle related to the P plane. (Based on refs. [10] and [16].)

tion in planes parallel and perpendicular to the hot-pressing axis, evaluating also grain size and grain morphology, correlating these results with mechanical properties.

## 2. Experimental procedure

Commercial  $\alpha$ - $\text{Si}_3\text{N}_4$  (H.C. Starck, LC-12),  $\text{Al}_2\text{O}_3$  (Baikalox, CR-6), and a mixed concentrate of yttrium and rare earth oxides,  $\text{CRE}_2\text{O}_3$ , produced at DEMAR-FAENQUIL, were used as starting powders. Previous works [17–19] have shown that the yttrium–rare earth oxide mixture,  $\text{CRE}_2\text{O}_3$ , is a solid solution consisting mainly of  $\text{Y}_2\text{O}_3$  (44%),  $\text{Yb}_2\text{O}_3$  (17%),  $\text{Er}_2\text{O}_3$  (14%) and  $\text{Dy}_2\text{O}_3$  (10%), and is an effective and cheap substitute for pure  $\text{Y}_2\text{O}_3$  as sintering additive for  $\text{Si}_3\text{N}_4$  ceramics, presenting similar sinterability and mechanical properties at room temperature. The total additive content was varied between 5 and 20 vol.%, maintaining a relationship of 60 mol% of  $\text{Al}_2\text{O}_3$  and 40 mol%  $\text{CRE}_2\text{O}_3$ .

Powder batches were produced by ball milling for 2 h using ethanol as milling media. After mixing, the powder batches were dried first in a rotary evaporator and subsequently in an oven at 120 °C for 12 h. Prior to hot-pressing the powder mixtures were sieved through a 60 mesh screen. Hot-pressing was done at 1750 °C for 30 min under a pressure of 20 MPa in nitrogen atmosphere, obtaining sintered specimen of approximately 20 mm diameter and 7 mm height.

The theoretical density of the samples was calculated according to the rule of mixtures and the final density after hot-pressing was measured by the immersion method in distilled water, using Archimedes' principle. The phase composition of the hot-pressed samples has been determined by X-ray diffraction, and the amount of phase transformation of  $\alpha$ - to  $\beta$ - $\text{Si}_3\text{N}_4$  was evaluated by the method proposed by Gazarra et al. [20]. For microstructural analysis by scanning electron microscopy (SEM) the hot-pressed specimens were cut and polished, and the surface was etched by a

molten mixture of NaOH and KOH in the proportion 1:1 at 500 °C during 1 to 3 min depending on the intergranular phase content.

The grain size distributions and aspect ratios were determined using the method proposed by Wötting et al. [2], based on the grains width and length measurements from SEM micrographs of polished sections perpendicular (normal—N) to the hot-pressing direction at 10,000 $\times$  magnification. This method depends on the statistic consideration that about 10% of the grains are cut parallel to their crystallographic  $c$ -axis and therefore show the realistic length and width of the elongated, rod-like  $\beta$ - $\text{Si}_3\text{N}_4$  grains. The average grain size is the mean value of 10% of the highest grain lengths observed, and by the length–width ratio of these grains the average aspect ratio has been determined.

Between 1000 and 1200 grains were measured using the software by LEICA Qwin-Image Processing and Analysis System for analysis, in order to obtain the average width, length and orientation of the grains. This orientation of the grains was evaluated by determining the angle  $\theta$  between the  $c$ -axis of the  $\beta$ - $\text{Si}_3\text{N}_4$  grains and the  $x$ -axis of the planes normal and parallel to the hot-pressing direction, see Fig. 1.

The hardness and fracture toughness were determined by Vicker's indentations [13–16], under an indentation load of 2 kg, for 30 s, in planes parallel (P) and normal (N) to the hot-pressing direction, as illustrated in Fig. 1. In plane P the toughness anisotropy was measured by aligning the two axes of the Vicker's indenter at angles of 0 and 90° in regard to the hot-pressing direction [12]. Twenty-one indentation measurements have been made for each value measured. Like this, the mean values and the standard deviation of the means are determined.

## 3. Results and discussion

### 3.1. Phase analysis and final density

The phase analysis of the hot-pressed specimen by X-ray diffraction (XRD) revealed only the presence of  $\beta$ - $\text{Si}_3\text{N}_4$  for

Table 1  
Microstructural characteristics of hot-pressed specimen (plane N)

Composition	Final relative density (%)	Average grain size ( $\mu\text{m}$ )	Planar grain density (no. of grains per $\mu\text{m}^2$ )	Aspect ratio
$\text{Si}_3\text{N}_4$ + 5 vol.% $\text{Al}_2\text{O}_3/\text{CRE}_2\text{O}_3$	$98.2 \pm 0.3$	$2.5 \pm 0.8$	1.28	$6.5 \pm 1.1$
$\text{Si}_3\text{N}_4$ + 10 vol.% $\text{Al}_2\text{O}_3/\text{CRE}_2\text{O}_3$	$98.5 \pm 0.2$	$2.9 \pm 0.9$	1.20	$9.5 \pm 1.4$
$\text{Si}_3\text{N}_4$ + 15 vol.% $\text{Al}_2\text{O}_3/\text{CRE}_2\text{O}_3$	$98.6 \pm 0.1$	$3.6 \pm 1.0$	1.01	$10.1 \pm 1.4$
$\text{Si}_3\text{N}_4$ + 20 vol.% $\text{Al}_2\text{O}_3/\text{CRE}_2\text{O}_3$	$98.0 \pm 0.2$	$4.1 \pm 1.0$	0.87	$11.2 \pm 1.5$

all compositions studied, indicating that the  $\alpha$ - to  $\beta$ - $\text{Si}_3\text{N}_4$  transition has been completed and, furthermore, that the additives formed an amorphous intergranular phase.

The relative densities of the samples after hot-pressing presented values higher than 98% for all compositions.

### 3.2. Microstructure

During liquid-phase sintering of  $\text{Si}_3\text{N}_4$  ceramics, the  $\alpha$ - $\text{Si}_3\text{N}_4$  grains dissolve in the liquid phase and precipitate in the form of elongated, hexagonal  $\beta$ - $\text{Si}_3\text{N}_4$  grains. The morphology (aspect ratio) depends to a large degree on the additives used and their quantity, under otherwise identical conditions (time, temperature, etc.). The results of the microstructural analysis of the hot-pressed samples of plane N, normal to the hot-pressing direction, are summarized in Table 1; listing the average grain sizes, the planar grain density, defined as number of grains per area, and the aspect ratio of the  $\beta$ - $\text{Si}_3\text{N}_4$  grains.

Besides the mean grain size listed in Table 1, Fig. 2 shows the cumulative grain size distributions of the  $\beta$ - $\text{Si}_3\text{N}_4$  grains for the four compositions studied with 5, 10, 15 and 20 vol.% of additives.

It is well known that the anisotropic growth of  $\beta$ - $\text{Si}_3\text{N}_4$  grains is related to the different growth rate on the basal plane and the lateral planes of the hexagonal  $\beta$ - $\text{Si}_3\text{N}_4$  prism. This behavior results in the atomic roughness difference between basal and lateral plane of the  $\beta$ - $\text{Si}_3\text{N}_4$  grains. In these

grains, the  $c$ -direction are not faceted, present higher roughness than prismatic planes (faceted). Like this, the growth rate in the  $c$ -axis is higher than in the  $a$ -axis, which leads to the anisotropic growth of these grains [22–24]. During hot-pressing, this effect of preferential grain growth is further enhanced by the applied pressure [25], resulting in grains of even higher aspect ratios, as shown in Table 1.

Furthermore, it can be observed that with increasing additive content larger grains are produced, due to the smaller degree of steric hinderance. In consequence, the planar grain density decreases with increasing additive content, as confirmed by the results listed in Table 1 and illustrated in Fig. 3. Furthermore, it can be observed that the aspect ratios of the  $\beta$ - $\text{Si}_3\text{N}_4$  grains increase with increasing additive content, from 6.5 to 11.2 for 5 and 20 vol.% additives, respectively, see Fig. 4. This result is explained by the higher grain growth velocity of the  $\beta$ - $\text{Si}_3\text{N}_4$  grains along their  $c$ -axis, when compared to the  $a$ - and  $b$ -axis, consistent with the work of Lee and Bowman [12].

In order to evaluate the anisotropy of the microstructure of these hot-pressed samples, the angles between the  $c$ -axis of the  $\beta$ - $\text{Si}_3\text{N}_4$  grains and the planes normal ( $\theta_N$ ) and parallel ( $\theta_P$ ) to the hot-pressing direction have been determined, as illustrated in Fig. 1. For a random orientation of the grains, the average angle should be  $45^\circ$  and the theoretical standard deviation  $25.98^\circ$ . The experimental results are summarized in Table 2, and shown graphically in Fig. 5. As can be observed, the grains in the plane normal to the hot-pressing direction are distributed randomly in respect to their orientation, resulting in angles  $\theta_N$  near  $45^\circ$  for all compositions studied, independently of the additive content.

On the other hand, in the plane parallel to the hot-pressing direction an alignment of the grains is observed, reflected by the angle  $\theta_P$ , inferior to  $45^\circ$  as expected for a random orientation. The angles  $\theta_P$  rise gradually with increasing additive

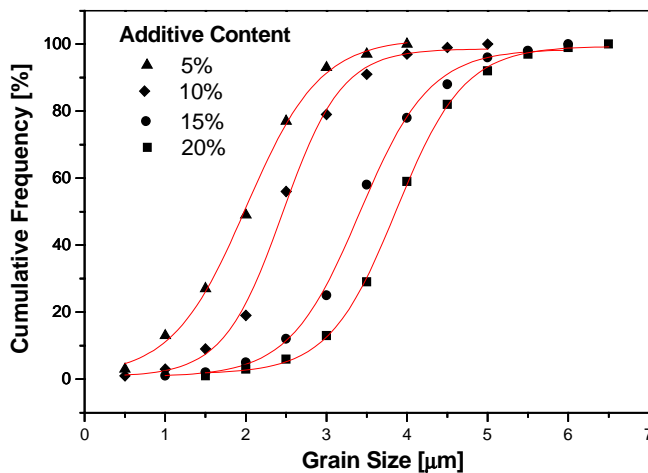


Fig. 2. Cumulative grain size distributions as function of the additive content.

Table 2

Orientation of grains in planes normal and perpendicular to the hot-pressing direction

Composition	Grains angle ( $\theta$ )	
	$\theta_N$ (N plane) ( $^\circ$ )	$\theta_P$ (P plane) ( $^\circ$ )
$\text{Si}_3\text{N}_4$ + 5 vol.% $\text{Al}_2\text{O}_3/\text{CRE}_2\text{O}_3$	$43.3 \pm 24.1$	$12.9 \pm 14.0$
$\text{Si}_3\text{N}_4$ + 10 vol.% $\text{Al}_2\text{O}_3/\text{CRE}_2\text{O}_3$	$46.4 \pm 23.5$	$25.9 \pm 19.6$
$\text{Si}_3\text{N}_4$ + 15 vol.% $\text{Al}_2\text{O}_3/\text{CRE}_2\text{O}_3$	$44.9 \pm 23.4$	$29.5 \pm 21.2$
$\text{Si}_3\text{N}_4$ + 20 vol.% $\text{Al}_2\text{O}_3/\text{CRE}_2\text{O}_3$	$44.5 \pm 20.8$	$35.1 \pm 23.5$

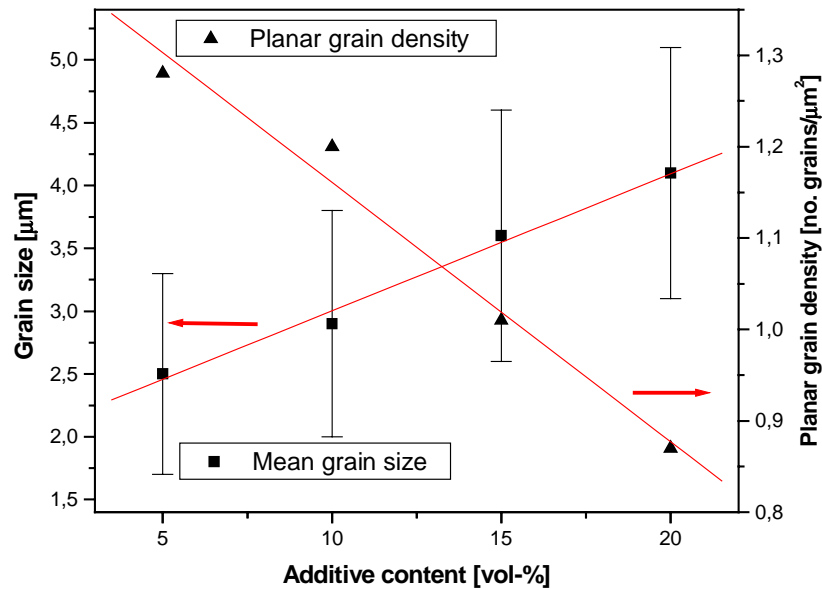


Fig. 3. Mean grain size and planar grain density as function of the additive content.

content, see Fig. 5, from 12.9 to 35.1° for an additive content of 5 and 20 vol.%, respectively, indicating a decreasing degree of orientation. This observation is further sustained by the increasing values of the standard deviation of the angle  $\theta_P$ . The alignment is less pronounced for higher additive contents, as can be clearly seen from Fig. 5, with a tendency towards random orientation, i.e. isotropic microstructure, for higher amounts of intergranular phase.

The alignment of the  $\beta$ - $\text{Si}_3\text{N}_4$  grains during hot-pressing is known to be the result of pressure gradients in planes parallel and perpendicular to the hot-pressing axis [12–26]. Therefore, the grains with  $c$ -planes perpendicular to the hot-pressing direction grow preferably. An X-ray diffraction technique commonly used to determine the anisotropy in planes parallel and perpendicular to the hot-pressing direc-

tion is based on the ratio of the peak areas between the (1 0 1) and (2 1 0) planes of the  $\beta$ - $\text{Si}_3\text{N}_4$  grains [12,26]. This technique has been shown to be very useful when analyzing the grain orientation of  $\text{Si}_3\text{N}_4$  ceramics with similar morphological characteristics, i.e. same aspect ratio and same average grain size. However,  $\text{Si}_3\text{N}_4$  ceramics sintered with different additive contents exhibit distinct morphological characteristics, turning this method unsuitable for a comparative analysis of the anisotropy of these materials. Therefore, we chose the direct determination of the grain orientation from SEM micrographs to evaluate quantitatively the microstructural anisotropy.

The results shown in Fig. 5 indicate that higher additive contents result in a decreasing difference between the average angles of the orientation in planes perpendicular ( $\theta_N$ )

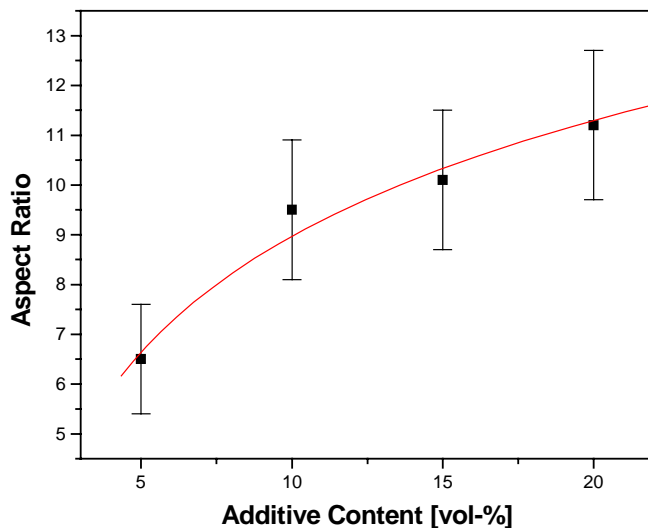


Fig. 4. Aspect ratio as function of the additive content.

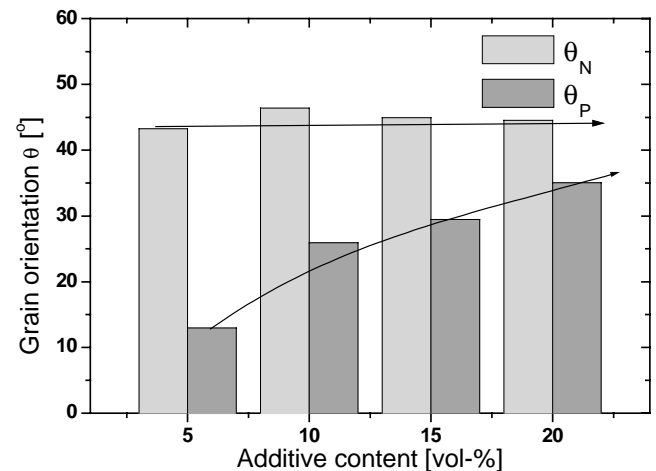


Fig. 5. Grain orientation as function of the additive content.  $\theta_N$ , average grain angle in the N plane;  $\theta_P$ , average grain angle in the P plane.

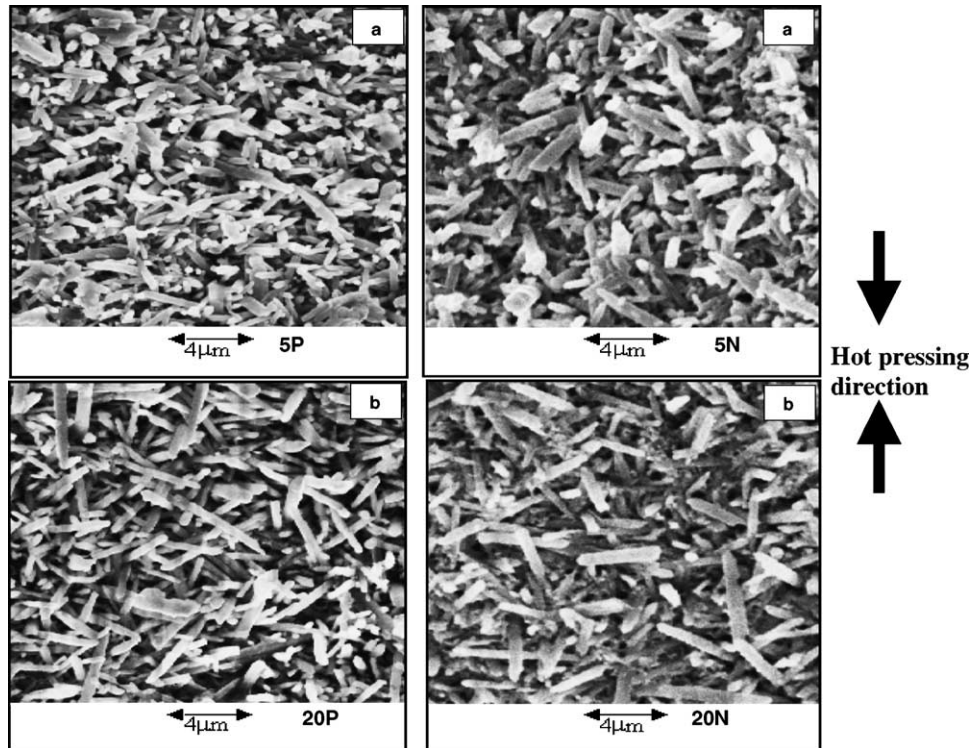


Fig. 6. Scanning electron micrographs of surfaces parallel (P) and normal (N) to the hot-pressing axis for (a) 5 vol.% and (b) 20 vol.% additives.

and parallel ( $\theta_P$ ) to the hot-pressing direction, as schematically shown in Fig. 1. This observation is in agreement with a possible grain rotation during hot-pressing as proposed by Yoon et al. [26] and steric hinderance effects. Higher additive contents result in enhanced growth velocities and at the same time in a lesser degree of steric hinderance. Furthermore, we suggest that with increasing additive contents rotation of grains at contact can take place more easily, and, consequently result in a smaller degree of anisotropy. These findings are document by the micrographs shown in Fig. 6 and illustrated in Fig. 7 for samples containing 5 and 20 vol.% additives.

### 3.3. Mechanical properties

The results of the Vicker's hardness, fracture toughness and its standard deviations, determined on the plane N, normal to the hot-pressing direction are summarized in Table 3.

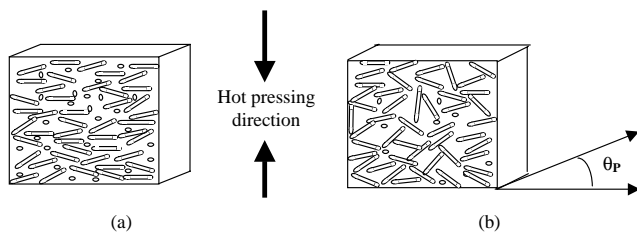


Fig. 7. Schematic orientation of  $\beta$ - $\text{Si}_3\text{N}_4$  grain growth in  $\text{Si}_3\text{N}_4$  hot pressed, in plane parallel to the hot-pressing axis: (a) 5 vol.%; (b) 20 vol.%.

As can be seen, the hardness decreases gradually with increasing additive content, because of the inferior hardness of the amorphous intergranular phase. This affirmation is supported by fact that, in all compositions (5–20 vol.% of  $\text{Al}_2\text{O}_3/\text{CRE}_2\text{O}_3$ ), no solid solution  $\text{Si}_3\text{N}_4$  ( $\text{SiAlON}$ ) are formed and the intergranular phase composition is not considerably altered. Like this, the increase of the additive content leads to the increase of the intergranular phase content and, consequently, to the decrease of the  $\beta$ - $\text{Si}_3\text{N}_4$  fraction in the mixture.

The fracture toughness increases with increasing additive content, consistent with the observation that increasing additive contents result in larger grains with higher aspect ratios, see Table 1, causing a higher degree of crack deflection and therefore higher toughness. No dependency of the fracture toughness on the orientation of the indentation mark has been found, signifying that plane N is isotropic in regard to the propagation of cracks, consistent with the random orientation of grains in this plane as shown in Table 2 and Fig. 5.

The results of the hardness measurements, fracture toughness and standard deviation, obtained by Vicker's

Table 3  
Hardness and fracture toughness (plane N)

Composition	Hardness (GPa)	$K_{IC}$ ( $\text{MPa m}^{1/2}$ )
$\text{Si}_3\text{N}_4$ + 5 vol.% $\text{Al}_2\text{O}_3/\text{CRE}_2\text{O}_3$	$16.28 \pm 0.32$	$5.9 \pm 0.2$
$\text{Si}_3\text{N}_4$ + 10 vol.% $\text{Al}_2\text{O}_3/\text{CRE}_2\text{O}_3$	$15.83 \pm 0.29$	$6.0 \pm 0.2$
$\text{Si}_3\text{N}_4$ + 15 vol.% $\text{Al}_2\text{O}_3/\text{CRE}_2\text{O}_3$	$15.12 \pm 0.24$	$6.3 \pm 0.3$
$\text{Si}_3\text{N}_4$ + 20 vol.% $\text{Al}_2\text{O}_3/\text{CRE}_2\text{O}_3$	$14.96 \pm 0.35$	$6.5 \pm 0.3$



Table 4  
Planar grain density, hardness and fracture toughness (plane P)

Composition	Planar grain density (no. of grains/ $\mu\text{m}^2$ )	Hardness (GPa)	Fracture toughness $K_{\text{IC}}$ ( $\text{MPa m}^{1/2}$ )			
			0°	90°	Average	$K_{\text{IC}}$ difference 0–90° (%)
$\text{Si}_3\text{N}_4$ + 5 vol.% $\text{Al}_2\text{O}_3/\text{Cr}_2\text{O}_3$	1.85	$15.86 \pm 0.28$	$6.6 \pm 0.5$	$5.2 \pm 0.2$	5.9	26.9
$\text{Si}_3\text{N}_4$ + 10 vol.% $\text{Al}_2\text{O}_3/\text{Cr}_2\text{O}_3$	1.63	$15.55 \pm 0.15$	$6.5 \pm 0.4$	$5.6 \pm 0.4$	6.1	16.1
$\text{Si}_3\text{N}_4$ + 15 vol.% $\text{Al}_2\text{O}_3/\text{Cr}_2\text{O}_3$	1.23	$14.68 \pm 0.24$	$6.4 \pm 0.4$	$5.8 \pm 0.4$	6.1	10.3
$\text{Si}_3\text{N}_4$ + 20 vol.% $\text{Al}_2\text{O}_3/\text{Cr}_2\text{O}_3$	1.12	$14.15 \pm 0.24$	$6.2 \pm 0.4$	$5.9 \pm 0.3$	6.1	5.1

indentation in plane P, separated into orientations of 0 and 90° in relation to the hot-pressing direction are listed in Table 4. As observed for plane N, the hardness also decreases with increasing additive content in plane P, because of the intergranular phase increase and consequently, reduction of the  $\beta\text{-Si}_3\text{N}_4$  fraction in the matrix. On the other hand a strong dependency of the fracture toughness on the direction in the plane P has been observed. For the direction parallel to the hot-pressing direction (0°), crack growth is effectively inhibited because of the preferential orientation of the elongated  $\beta\text{-Si}_3\text{N}_4$  grains at approximately 90°. For the other direction of 90°, substantially lower fracture toughness values have been measured. The fracture toughness determined for the two directions differs up to 27% for the composition with the lowest additive content of 5 vol.% and gradually diminishes with increasing additive content to approximately 5% for samples with 20 vol.% additives as shown in Fig. 8, because of the decreasing degree of grains orientation in this plane. Two examples of the dependency of crack length on orientation are shown in Fig. 9 for specimen with 5 and 20 vol.% of additives.

The hardness and average fracture toughness values of plane P are inferior to those determined for plane N, probably because of the smaller planar grain density of plane P in relation to plane N.

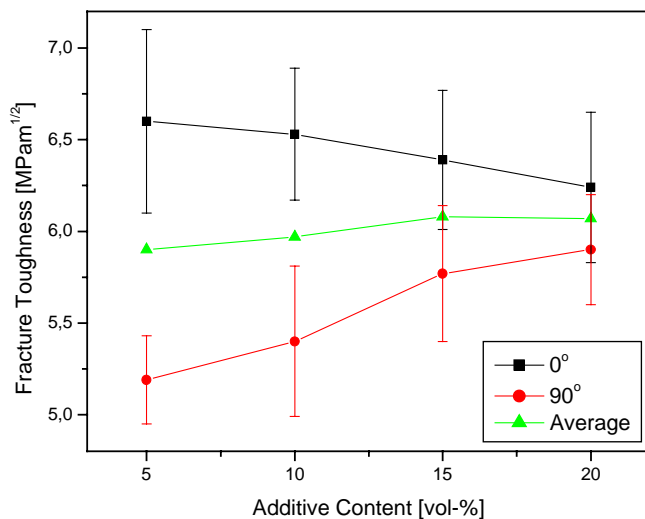


Fig. 8. Anisotropy of fracture toughness (plane P) in relation of additive content.

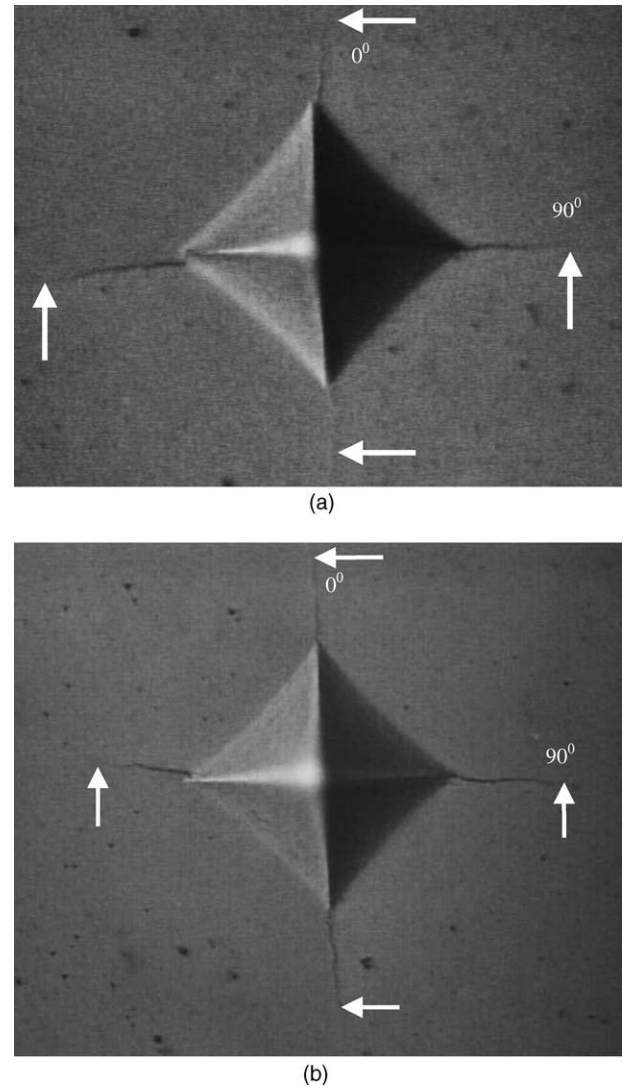


Fig. 9. Vicker's indentation marks orientated at 0 and 90° to the hot-pressing direction in plane P. (a) 5 vol.% additives and (b) 20 vol.% additives.

#### 4. Conclusions

It has been shown that the direct determination of the orientation of the  $\beta\text{-Si}_3\text{N}_4$  grains by analysis of SEM micrographs is a simple and reliable technique to determine the anisotropy of hot-pressed  $\text{Si}_3\text{N}_4$  ceramics, permitting a

comparison of microstructures composed of grains with different sizes and aspect ratios, as well as changing amounts of intergranular secondary phases. In planes normal to the hot-pressing direction no preferential orientation of the grains has been found, independent of the additive content. In planes parallel to the hot-pressing direction, a preferential orientation of the grains has been verified, depending strongly on the additive content. With increasing additive content a tendency for a random orientation of the grains is observed.

The preferential orientation of the grains reflects also in the variation of the mechanical properties, especially fracture toughness. Fracture toughness values varied up to 27% for  $\text{Si}_3\text{N}_4$  with an additive content of 5 vol.% in planes normal and perpendicular in regard to the hot-pressing direction. This difference is gradually reduced with increasing additive content to only 5% for an additive content of 20 vol.%, due to a lesser degree of steric hinderance and grain rotation. Crack propagation is effectively hindered in directions perpendicular to the grain orientation, causing higher fracture toughness in these directions.

## Acknowledgements

This work received financial support by FAPESP under Grant no. 01/08682-6.

## References

- [1] A.J. Pyzik, D.R. Braman, Microstructure and properties of self-reinforced silicon nitride, *J. Am. Ceram. Soc.* 76 (6) (1993) 2737–2744.
- [2] G. Wötting, B. Kanka, G. Ziegler, Microstructural characterization, and relation to mechanical properties of dense silicon nitride, in: S. Hampshire (Ed.), *Non-Oxide Technical and Engineering Ceramics*, Elsevier, London, UK, 1986, pp. 83–96.
- [3] E. Tani, S. Umabayashi, K. Kishi, K. Kobayashi, M. Nishijima, Gas-pressure sintering of  $\text{Si}_3\text{N}_4$  with concurrent addition of 5 wt.% rare-earth oxide: high fracture toughness  $\text{Si}_3\text{N}_4$  with fiberlike structure, *Am. Ceram. Soc. Bull.* 65 (9) (1986) 1311–1315.
- [4] P.F. Becher, E.Y. Sun, K.P. Plucknett, K.B. Alexander, C.-H. Hsueh, H.-T. Lin, S.B. Waters, C.G. Westmoreland, Microstructural design of silicon nitride with improved fracture toughness. I. Effects of grain shape and size, *J. Am. Ceram. Soc.* 81 (11) (1998) 2821–2830.
- [5] S. Kanzaki, M.E. Brito, M.C. Valecillos, K. Hirao, M. Toriyama, Microstructure designing of silicon nitride, *J. Eur. Ceram. Soc.* 17 (1997) 1841–1947.
- [6] P.F. Becher, Microstructural design of toughened ceramics, *J. Am. Ceram. Soc.* 74 (2) (1991) 255–269.
- [7] A. Bellosi, Design and process of non-oxide ceramics, Case study: factors affecting microstructure and properties of silicon nitride, in: Y.G. Gogotsi, R.A. Andreievski (Eds.), *Materials Science of Carbides, Nitrides and Borides*, Kluwer Academic Publishers, The Netherlands, 1999, pp. 285–304.
- [8] F.L. Riley, Silicon nitride and related materials, *J. Am. Ceram. Soc.* 83 (2) (2000) 245–265.
- [9] K.T. Faber, A.G. Evans, Crack deflection processes. I. Theory, *Acta Metall.* 31 (4) (1983) 565–576.
- [10] H. Kitagawa, R. Yukki, T. Ohira, Crack-morphological aspects in fracture mechanics, *Eng. Fract. Mech.* 7 (1975) 515–529.
- [11] J.W. Hutchinson, Crack tip shielding by micro-cracking in brittle solids, *Acta Metall.* 35 (7) (1987) 1605–1619.
- [12] F. Lee, K.J. Bowman, Texture and anisotropy in silicon nitride, *J. Am. Ceram. Soc.* 75 (7) (1992) 1748–1755.
- [13] D.S. Park, C.W. Kim, Indentation crack length anisotropy in silicon nitride with aligned reinforced grains, *J. Am. Ceram. Soc.* 83 (3) (2000) 663–665.
- [14] J.C. Hay, E.Y. Sun, G.M. Pharr, P.F. Becher, K.B. Alexander, Elastic anisotropy of  $\beta$ -silicon nitride whiskers, *J. Am. Ceram. Soc.* 81 (10) (1998) 2661–2669.
- [15] T. Ohji, K. Hirao, S. Kanzaki, Fracture resistance behavior of highly anisotropic silicon nitride, *J. Am. Ceram. Soc.* 78 (11) (1995) 3125–3128.
- [16] A.G. Evans, E.A. Charles, Fracture toughness determination by indentation, *J. Am. Ceram. Soc.* 59 (7/8) (1976) 371–372.
- [17] K. Strecker, R. Gonzaga, S. Ribeiro, M.J. Hoffmann, Substitution of  $\text{Y}_2\text{O}_3$  by a rare earth oxide mixtures as sintering additive of  $\text{Si}_3\text{N}_4$  ceramics, *Mater. Lett.* 45 (2000) 39–42.
- [18] C. Santos, S. Ribeiro, K. Strecker, C.R.M. Silva, Substitution of pure  $\text{Y}_2\text{O}_3$  by a mixed concentrate of rare earth oxides ( $\text{Ce}_2\text{O}_3$ ) as sintering additive of  $\text{Si}_3\text{N}_4$ : a comparative study of the mechanical properties, *J. Mater. Process. Technol.* 142 (2003) 697–701.
- [19] C. Santos, K. Strecker, S.A. Baldacim, O.M.M. Silva, C.R.M. Silva, Mechanical properties improvement related to the isothermal holding time in  $\text{Si}_3\text{N}_4$  ceramics sintered with an alternative additive, *Int. J. Refract. Met. Hard Mater.* 21 (2003) 245–250.
- [20] C.D. Gazarra, D.R. Messier, Determination of phase content of  $\text{Si}_3\text{N}_4$  by X-ray diffraction analysis, *Ceram. Bull.* 56 (9) (1977) 777–780.
- [21] T. Hansson, R. Warren, J. Wasén, Fracture toughness anisotropy and toughening mechanisms of a hot-pressed alumina reinforced with silicon carbide whiskers, *J. Am. Ceram. Soc.* 76 (4) (1993) 841–848.
- [22] M. Kitayama, K. Hirao, M. Toriyama, S. Kanzaki, Modeling and simulation of grain growth in  $\text{Si}_3\text{N}_4$ . I. Anisotropic Ostwald ripening, *Acta Mater.* 46 (18) (1998) 6541–6550.
- [23] H. Björklund, L.N.L. Falk, K. Rundgren, J. Wasén,  $\beta$ - $\text{Si}_3\text{N}_4$  grain growth. Part I. Effect of metal oxide sintering additives, *J. Eur. Ceram. Soc.* 17 (1997) 1285–1299.
- [24] M. Herrmann, I. Schulz, W. Hermel, Chr. Schubert, A. Wendt, Some new aspects of microstructural design of  $\beta$ - $\text{Si}_3\text{N}_4$  ceramics, *Z. Metallkd.* 92 (7) (2001) 788–795.
- [25] R.L. Coble, Diffusion models for hot pressing with surface energy and pressure effects as driving forces, *J. Appl. Phys.* 41 (12) (1970) 4798–4807.
- [26] S.Y. Yoon, T. Akatsu, E. Yasuda, Anisotropy of creep deformation rate in hot-pressed  $\text{Si}_3\text{N}_4$  with preferred orientation of the elongated grains, *J. Mater. Sci.* 32 (1997) 3813–3819.